Revista Mexicana de Astronomía y Astrofísica, **60**, 83–98 (2024)

https://doi.org/10.22201/ia.01851101p.2024.60.01.06

CCD PHOTOMETRY OF THE GLOBULAR CLUSTER NGC 5897[1]

A. Ruelas-Mayorga[2], L. J. Sánchez[2], E. Macías-Estrada[2], and A. Nigoche-Netro[3]

Received September 12 2023; accepted November 1 2023

ABSTRACT

We report CCD photometric observations of the globular cluster NGC 5897, in the Johnson system filters B, V, R, and I. With the values for these magnitudes we obtain various colour indices and produce several colour-magnitude diagrams. We present eight colour-magnitude diagramas: V vs $B-V$, B vs $B-V$, V vs $V-I$, I vs $V-I$, R vs $R-I$, I vs $R-I$, V vs $V-R$, and R vs $V-R$. In all of these diagrams we can clearly see the giant branch, the horizontal branch and the beginning of the main sequence. To the left of the main sequence turn-off point we detect a somewhat large number of blue straggler stars. We determine the mean value of the visual magnitude of the HB as 16.60 ± 0.46. This value is fainter than the value found by other authors.

RESUMEN

Se reportan observaciones fotométricas del cúmulo globular NGC 5897 en los filtros del sistema de Johnson B, V, R e I. Con los valores de estas magnitudes obtenemos diferentes índices de color y producimos varios diagramas color-magnitud. Presentamos ocho diagramas color-magnitud V vs $B-V$, B vs $B-V$, V vs $V-I$, I vs $V-I$, R vs $R-I$, I vs $R-I$, V vs $V-R$, y R vs $V-R$. En todos estos diagramas se distinguen claramente la rama de las gigantes, la rama horizontal y el comienzo de la secuencia principal. A la izquierda del punto de salida de la secuencia principal detectamos un número relativamente grande de estrellas '*blue stragglers*'. Determinamos el promedio de la magnitud visual de la rama horizontal como 16.60 ± 0.46. Este valor es más débil que el valor encontrado por otros autores.

Key Words: Galaxy: general — globular clusters: individual: NGC 5897 — techniques: photometric

1. INTRODUCTION

The globular clusters are spherically symmetric stellar systems which may be found in all galaxies. They are very rich stellar systems that may be found in our Galaxy in remote regions of the galactic halo and also close to the galactic centre. They contain hundreds of thousands of stars within a radius $20-50$ pc, having typical central densities between 10^2 and 10^4 stars/pc^3. Globular clusters are dynamically very stable and may live for a long time. They represent a remnant of a primordial stellar formation epoch and may be considered as proper galactic subsystems (Ruelas-Mayorga et al. 2010).

Many Milky Way globular clusters have been known for a long time (see the Messier (1771) catalogue). Presently we think there are approximately 150-200 in our Galaxy, although this figure does not include those clusters close to the galactic plane or very low surface brightness objects, (see Monella (1985) and Harris (1996)).

Because globular clusters are very luminous systems they may be observed at very large distances. This fact makes them fundamental in the study of galactic structure.

Some characteristics of globular clusters are:

- In general, the light that comes from these objects originates in stars slightly cooler than our Sun.

[1]Based upon observations acquired at the Observatorio Astronómico Nacional on the Sierra San Pedro Mártir (OAN-SPM), Baja California, México.

[2]Instituto de Astronomía, Universidad Nacional Autónoma de México, CDMX, México.

[3]Instituto de Astronomía y Meteorología, Universidad de Guadalajara, Guadalajara, Jal. 44130, México.

- Morphology. In general, they are slightly elliptical in shape. The average ratio between the minor and major axes of the apparent ellipse that they project on the sky is $b/a = 0.73$, with only 5% of them more elongated than $b/a = 0.8$.
- They appear to be exclusively stellar system in which no presence of gas or dust is detected (Binney & Merrifield 1998).
- The radial distribution of stars varies between clusters, and there are some that present a strong central concentration (Mihalas & Binney 1981).
- The value of their integrated absolute magnitude $(M_V)_0$ is usually found in the interval $-5 >(M_V)_0 \gtrsim -10$ where the maximum of the distribution is found at $(M_V)_0 \approx -8.5$ and with a FWHM of $\approx \pm 1$ mag.
- Their intrinsic colour takes values in the interval $0.4 \lesssim (B-V)_0 \lesssim 0.8$ with a maximum at $(B-V)_0 \approx 0.57$ (Mihalas & Binney 1981).
- There are clusters with a large metallic deficiency, usually located in the galactic halo, up to those with abundances similar to that of the Sun (Mihalas & Binney (1981), Harris (2010), Pfeffer et al. (2023)).
- It is common to find clusters with metallic abundances in the interval $-2.2 \lesssim [Fe/H] \lesssim 0.0$.

Studies of globular clusters are important because they serve a variety of astronomical purposes, such as: determination of the galactic centre position, as indicators of the galactic gravitational potential (i.e. Ishchenko et al., 2023 and references therein), studies of the evolution of low mass and low metallicity stars, and also of chemical evolution of galactic systems. Globular clusters can also provide restrictions on galaxy formation (i.e. Strader et al. (2005), Harris et al. (2013), Beasley (2020), and Palma (2023)).

NGC 5893 is a low concentration cluster ($c = \log\ r_t/r\ c = 1.19$) Webbink (1985). There are in the literature several published colour-magnitude diagrams for this cluster (Sandage & Katem (1968), Sarajedini (1992), Ferraro et al. (1992) and Stetson (2019)). Sandage & Katem (1968) obtained B and V photometry down to $V \approx 17$ which was just able to include the horizontal branch (HB) of this cluster. They found that $V(HB) = 16.20$, $E(B-V) = 0.11 \pm 0.02$ and $(B-V)_{0,g} = 0.78 \pm 0.03$ (the dereddened colour of the giant branch (GB) at the level of the HB), this allowed them to determine the metallicity of NGC 5893 to be between that of M3 and M92. The HB of this cluster is made mainly of blue stars. Wehlau (1990) found the average of the V magnitude of the RR Lyrae star in this cluster to be $V(\mathrm{RR}) = 16.30$. Sarajedini (1992) obtained CCD B and V photometry of this cluster down to $V \approx 22$. In this paper he reached the following conclusions:

- The HB of this cluster appears to be made mainly by blue stars with $V(\mathrm{HB}) = 16.35 \pm 0.15$.
- The metallicity of this cluster is $[\mathrm{Fe/H}] = -1.66 \pm 0.10$. He obtains this value from his adopted value for the $E(B-V) = 0.07 \pm 0.04$, and the colour of the red giant branch (RGB) at the level of the HB.
- He finds that NGC 5897 is ≈ 2 Gyr older that the globular cluster M3.
- The luminosity function of the RGB shows an enhancement of the number of stars at the level of the HB.
- The colour-magnitude (CM) diagram of this cluster reveals a large population of blue straggler stars.

This paper is organised as follows: in § 2 we present the observations and describe the reduction of the standard stars, in § 3 the reduction of the photometry of the cluster stars is described, as well as the procedure for aligning and matching the different sections of the cluster which we observed. § 4 deals with the derivation of the fiducial lines and the introduction of the colour-magnitude diagrams, the following section (§ 5) presents the different colour-magnitude diagrams which we derived. § 6 talks about the calculation of the metallicity and the reddening using the Sarajedini & Layden method (see Sarajedini (1994) and Sarajedini & Layden (1997)). § 7 derives the distance modulus to NGC 5897, and finally, in § 8 we present our conclusions.

2. THE OBSERVATIONS

The globular cluster NGC 5897 is located on the constellation of Libra ($AR(2000: 15^h17^m24.5^s$, $DEC(2000: -21°00'37.0'')$), it contains several hundred thousands stars (see Figure 1). Its most important properties are listed in Table 1 (Harris 1996).

We obtained the observations at the Observatorio Astronómico Nacional in San Pedro Mártir (OAN-SPM), Baja California during 2006, March 20-23 and 2007, March 14.

TABLE 1

Data for the Globular Cluster NGC 5897

Right Ascension (2000)		$15^h17^m24.5^s$
Declination (2000)		$-21^o00'37.0''$
Galactic Longitude		342.95
Galactic Latitude		30.29
Distance to the Sun(kpc)		12.5
Tidal radius (arcmin) (Webbink 1985)		11.5
Distance to the Galactic Centre (kpc)		7.4
Reddening $E(B-V)$		0.09
Horizontal Branch Magnitude (in V)		16.27
Distance Modulus $(m-M)$ (in V)		15.76
Integrated V Magnitude		8.53
Absolute Visual Magnitude		-7.23
	$U-B$	0.08
Integrated Colour Indices	$B-V$	0.74
(no reddening correction)	$V-R$	0.50
	$V-I$	1.041
Metallicity [Fe/H]		-1.90
Integrated Spectral Type		$F7$
Heliocentric Radial Velocity (km/s)		101.5
Central Concentration		0.86
Ellipticity		0.08
Nucleus Radius (arcmin)		1.40
Mean Mass Radius (arcmin)		2.06
Central Surface Brightness (in V) (magnitudes/arcsec)		20.53
Logarithm of the luminous density at the centre $(L_\odot/\mathrm{pc}^3)$		1.53

Fig. 1. The globular cluster NGC 5897. The image is 12.6′ vertically (Taken from: `http://astrim.free.fr/ngc5897.htm/`).

We utilised two different CCD cameras attached to the 1.5 m telescope. The characteristics of these detectors are presented in Table 2.

As stated above, the observations were collected during two observing runs, during which, we observed in a standard way obtaining bias and flat field frames in each filter, plus obtaining multiple observations of standard star regions. In Tables 3 and 4 we present the logs for both observation seasons regarding the globular cluster NGC 5897.

2.1. *Reduction of Standard Stars*

In order to express the magnitude of the stars in the globular cluster in a standard system, we performed aperture photometry of stars in some of the Landolt Standard Regions (Landolt 1992) listed in Tables 3 and 4. The photometric observations of the standard stars was carried out using the APT (Aperture Photometry Tool) (Laher et al. 2012), (see also `https://www.aperturephotometry.org/about/`).

The APT programme is a software that permits aperture photometry measurements of stellar images on a frame. The programme accepts images in the *fits* format, so no transformation of our images to other formats was necessary. The standard regions which were measured had already been processed by

TABLE 2

Characteristics of the Detectors Used in the Observations		
Characteristic	Thomson	Site1
Size (pixels)	2048×2048	1024×1024
Pixel Size (μm)	14×14	24×24
Quantum Efficiency	Maximum 65% at 5000 Å	
Reading noise (e^-) (gain mode 4 binning 2×2)	5.3	5.5 (Direct Imaging)
Dark Current (e^-/pix/h)	1.0 a $-95.2^o C$	7.2 approximately at -80° C
Well Depth (e^-)	1.23×10^5 (MPP Mode)	
Bias Level (gain mode 4 binning 2×2)	384	547 (Direct Imaging)
Gain (e^-) (Mode 4)	0.51	1.27
A/D Converter	16 bits	
Linearity	99%	99.5%
Plate Scale ($''$/pixel)	0.147	0.252

removal of hot and cosmic ray pixels, and were bias and flat-field corrected.

We propose a set of transformation equations from the observed to the intrinsic photometric system that looks as follows:

$$B_{int} - B_{obs} = A_B * X + K_B * (B-V)_{obs} + C_B, \quad (1)$$

$$V_{int} - V_{obs} = A_V * X + K_V * (B-V)_{obs} + C_V, \quad (2)$$

$$R_{int} - R_{obs} = A_R * X + K_R * (R-I)_{obs} + C_R, \quad (3)$$

$$I_{int} - I_{obs} = A_I * X + K_I * (R-I)_{obs} + C_I, \quad (4)$$

where the suffixes *int* and *obs* stand for *intrinsic* and *observed*, and A, K and C correspond to the negative of the atmospheric absorption coefficient, the colour term and the zero point term. These are the terms that we intend to calculate using the intrinsic values for the magnitudes given in Landolt (1992), and the observed values measured with APT. The equations are solved using the least squares procedure and the coefficients obtained are shown in Tables 5, 6, 7 and 8.

In Figure 2 we plot, for magnitudes B, V, R and I, on the vertical axis the difference between the intrinsic magnitude of the standard stars and their calculated values using the transformation equations (equations 1, 2, 3 and 4) given above, and on the horizontal axis we plot the corresponding observed value for the magnitude. It is clear from these graphs that the calculated values minus the intrinsic values of the magnitudes for the standard stars are, in its majority, distributed around the zero value. However, there are two groups of stars that differ significantly from zero and appear displaced above and below the rest of the stars. These anomalous stars belong in general to the regions PG0942, Rubin 152, PG 1323 and Area 98. We have checked that the stars in these regions are well identified with our observation frames. However, we have been unable to find the cause of this discrepancy; therefore, these anomalous stars were eliminated from the rest of the analysis.

The reduction of the data was done in a standard way, that is, removing dead and hot pixels produced by cosmic rays, and performing bias subtraction, and flat field correction. This reduction process was achieved using the general purpose software: Image Reduction and Analysis Facility (IRAF). Once the fields have been bias and flat field corrected we proceed to utilise the routine DAOPHOT to obtain the photometry of the many starts present in the field using the Point Spread Function (PSF) technique (Stetson 1992). As an example of an image on which we apply the DAOPHOT technique see Figure 3.

Figure 4 show graphs of the measurement errors as function of the value of the observed magnitude for B, V, R and I. It is clear that for brighter magnitudes the measurement errors are very small and begin to increase as we move to fainter magnitudes, becoming of the order of several tenths of magnitude by a magnitude value of ≈ 20.

3. PHOTOMETRY OF THE CLUSTER STARS

The calculation of the different observed magnitudes of the stars in the cluster NGC 5897 was obtained by a standard application of the DAOPHOT subroutine present in IRAF to all the observed frames in each filter, after having the frames bias-subtracted and flat fielded.

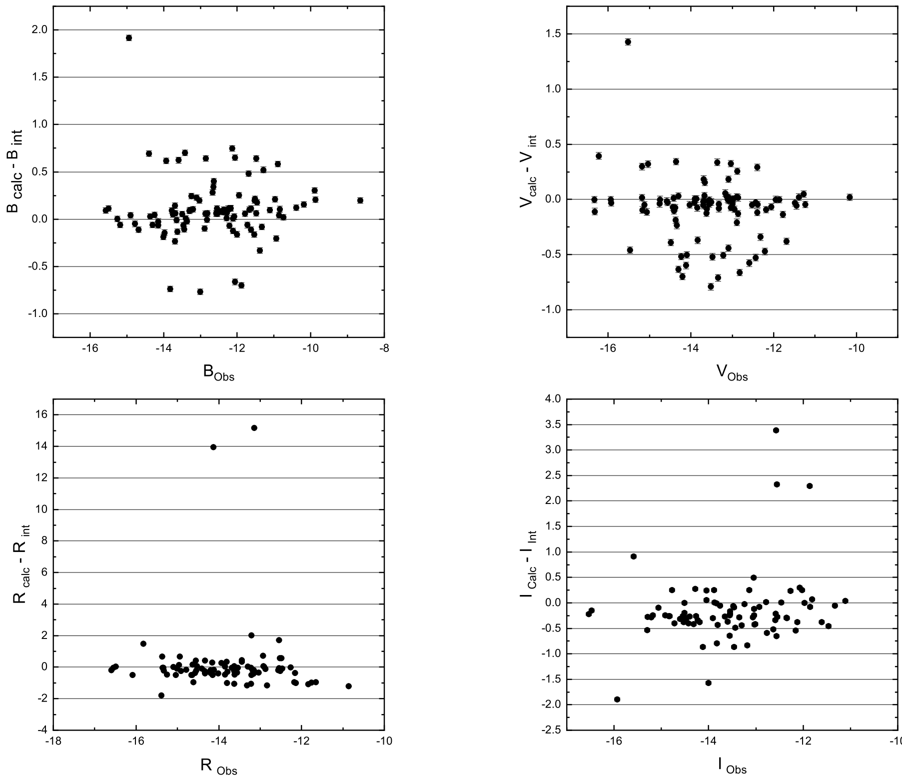

Fig. 2. Calculated minus intrinsic magnitude versus observed magnitude.

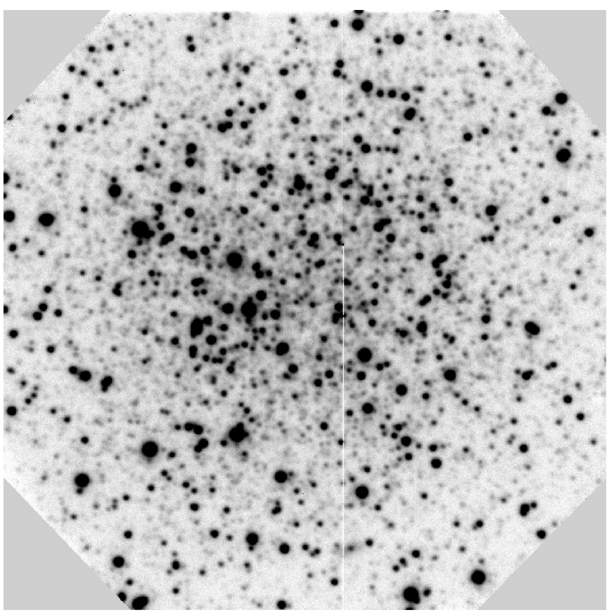

Fig. 3. Image of the central zone of the globular cluster NGC 5897 in the R filter after the process of preparation.

The magnitude catalogues produced by the subroutine ALLSTAR for the observations were combined to obtained the observed colours for the stars in the globular cluster, so that the application of equations 1, 2, 3 and 4 with the appropriate transformation coefficients was straightforward.

3.1. *Colour-Magnitude Diagrams*

In order to construct the colour-magnitude diagrams we utilised the photometric catalogues, in the four filters of interest B, V, R and I, which were derived from the application of the DAOPHOT subroutines. The diagrams which we shall present are the following: (B vs $B-V$), (V vs $B-V$), (V vs $V-I$), (I vs $V-I$), (I vs $R-I$), (R vs $R-I$), (V vs $V-R$) and (R vs $V-R$). To be able to use the derived photometric catalogues, it is necessary to effect a series of steps so that the frames in all filters are compatible. It was therefore necessary to align, group, and standardise them as well as eliminate those stars that might appear repeated.

3.2. *Alignment*

To obtain the colours of the star in NGC 5897 we need to pair the different magnitude catalogues. This procedure is not a trivial one since one star does not necessarily have the same coordinates in all the frames in which it appears. We have to remember that each filter observation was taken in 5 different frames (North, South, East, West and Centre) which have to be assembled into a grand image

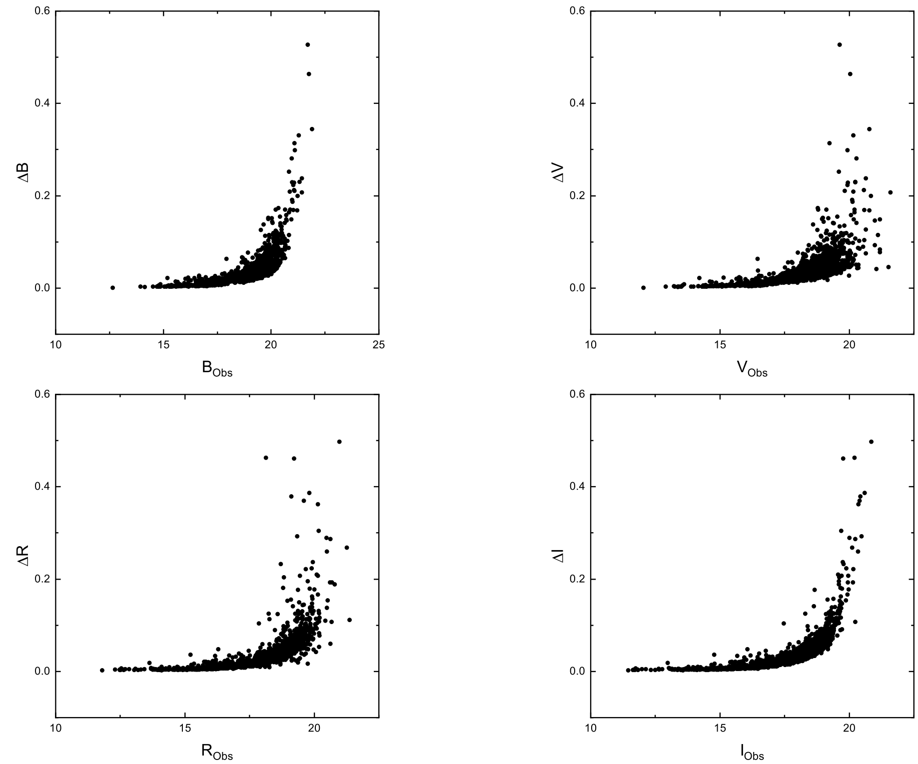

Fig. 4. Measurement error ΔMag vs Mag_{Obs} for B, V, R and I.

for the entire cluster, taking care to obtain the average of the intensity of those stars that appear on any two sections of the mosaic. Taking into consideration that we used one CCD in 2006 and a different one in 2007 the matching of the images required a positional transformation which consisted of a translation, a rotation and a stretching. Fortunately, the coefficients for rotation and stretching resulted in very small numbers, so our problem reduced itself to a simple translation of coordinates. We define as a primary reference frame the positions and the magnitudes of the stars in the central image observed for the 2007 observing season. Doing this, we ended up having photometric files for the four filters in the same positional and magnitude systems, which allowed the calculation of colours in an easy and straightforward way.

4. PHOTOMETRY OF THE STARS IN NGC 5897, COLOUR CATALOGUES AND FIDUCIAL LINES

The standard magnitudes for the stars in the cluster NGC 5897 were obtained by comparison with the published photometry results for this cluster published by Stetson (2019). A number of stars were identified in our and Stetson's observations, and a linear transformation between one set of observations and the other was proposed as follows:

$$\alpha = C_1 X_{pos} + C_2 \ , \qquad (5)$$

where α represents right ascension, C_1 is the longitudinal stretching coefficient, X_{pos} represents the X coordinate value in our files and C_2 is the longitudinal coefficient of translation.
Analogously,

$$\delta = C_3 Y_{pos} + C_4 \ , \qquad (6)$$

where δ represents the declination, C_3 is the transversal stretching coefficient, Y_{pos} represents the Y coordinate in our files and C_4 is the transversal coefficient of translation.

The values we obtained for the transformation coefficients between our positions and those of Stetson's are as follows:

- $C_1 = -9.60592 \times 10^{-5}$
- $C_2 = 229.39920$
- $C_3 = 8.76398 \times 10^{-5}$
- $C_4 = -21.06008$

TABLE 3

Observation log for March 2006		
Object Observed	Filter	Number of Images
Bias		5
Flat Field *B*	*B*	5
Flat Field *V*	*V*	5
Flat Field *R*	*R*	5
Flat Field *I*	*I*	5
Region 98	*B*	4
Region 98	*V*	4
Region 98	*R*	4
Region 98	*I*	4
Rubin 152	*B*	4
Rubin 152	*V*	4
Rubin 152	*R*	4
Rubin 152	*I*	4
Rubin 149	*B*	4
Rubin 149	*V*	4
Rubin 149	*R*	4
Rubin 149	*I*	4
PG 1323	*B*	4
PG 1323	*V*	4
PG 1323	*R*	4
PG 1323	*I*	4
PG 0942	*B*	4
PG 0942	*V*	4
PG 0942	*R*	4
PG 0942	*I*	4
PG 1525	*B*	4
PG 1525	*V*	4
PG 1525	*R*	4
PG 1525	*I*	4
PG 1528	*B*	4
PG 1528	*V*	4
PG 1528	*R*	4
PG 1528	*I*	4
NGC 5897	*B*	10
NGC 5897	*V*	10
NGC 5897	*R*	10
NGC 5897	*I*	10

The magnitude transformation results simply on an additional displacement for the four filters. This procedure is applied to our four mosaics in filters *B*,

TABLE 4

Observation log for March 2007		
Object Observed	Filter	Number of Images
Bias		10
Flat Field *B*	*B*	3
Flat Field *V*	*V*	3
Flat Field *R*	*R*	3
Flat Field *I*	*I*	3
Rubin 152	*B*	3
Rubin 152	*V*	3
Rubin 152	*R*	3
Rubin 152	*I*	3
Rubin 149	*B*	3
Rubin 149	*V*	3
Rubin 149	*R*	3
Rubin 149	*I*	3
PG 1323	*B*	3
PG 1323	*V*	3
PG 1323	*R*	3
PG 1323	*I*	3
PG 0942	*B*	3
PG 0942	*V*	3
PG 0942	*R*	3
PG 0942	*I*	3
PG 1525	*B*	3
PG 1525	*V*	3
PG 1525	*R*	3
PG 1525	*I*	3
NGC 5897 C, N, E, W	*B*	10
NGC 5897 C, N, E, W	*V*	10
NGC 5897 C, N, E, W	*R*	10
NGC 5897 C, N, E, W	*I*	10

TABLE 5

Standard System	A_B	K_B	C_B
21-22 March 2006	-0.36496	0.19409	26.83682
22-23 March 2006	-1.23555	0.17829	26.39759
23-24 March 2006	-0.41733	0.42103	26.78603
12-13 March 2007	1.16919	0.10874	25.34031
13-14 March 2007	-0.30223	0.10583	27.47228
14-15 March 2007	-0.37970	0.13717	27.53140

TABLE 6

Standard System	A_V	K_V	C_V
21-22 March 2006	0.94214	0.05596	25.03835
22-23 March 2006	-1.67073	0.00563	28.07604
23-24 March 2006	-0.46776	0.30053	27.38143
12-13 March 2007	0.12127	-0.02352	27.58167
13-14 March 2007	-0.25039	-0.03984	27.76332
14-15 March 2007	-0.32799	-0.02824	27.86426

TABLE 7

Standard System	A_R	K_R	C_R
21-22 March 2006	—	—	—
22-23 March 2006	-1.83264	0.13357	28.60749
23-24 March 2006	-0.59665	0.50853	27.63788
12-13 March 2007	0.37819	-0.02996	27.22330
13-14 March 2007	-0.13806	-0.04880	27.22305
14-15 March 2007	-0.23895	-0.05205	27.75572

TABLE 8

Standard System	A_I	K_I	C_I
21-22 March 2006	—	—	—
22-23 March 2006	-2.25859	0.14873	29.11512
23-24 March 2006	-0.56102	0.78455	27.07607
12-13 March 2007	1.14735	0.06524	25.31618
13-14 March 2007	-0.02309	0.00138	26.50840
14-15 March 2007	0.11989	-0.02645	26.57065

V, R and I producing a final set of NGC 5897 stars in four filters on a standard system of position and magnitude.

4.1. *Colour Catalogues*

We formed four colour catalogues as follows:

- $B - V$ catalogue: 1656 stars
- $V - I$ catalogue: 1935 stars
- $R - I$ catalogue: 2026 stars
- $V - R$ catalogue: 2587 stars

The number of stars in each catalogue is different because not all stars are equally detected in the different filters and therefore, some of them may be detected in one filter and not in another.

4.2. *Fiducial Lines (FL) and Colour-Magnitude Diagrams (CMD)*

In this section we shall present the colour magnitude diagrams which we obtained from the photometry performed on the stars of the globular cluster NGC 5897. Each colour-magnitude diagram will be presented as a plot of magnitude versus colour, on which we have superimposed a series of lines which correspond to the fiducial line for the giant branch and part of the main sequence. The fiducial line was obtained with the following procedure:

- We calculate the maximum and minimum value of the magnitude interval.
- We divide this interval in a number of magnitude bins.
- Along each magnitude bin we find the number of stars in a number of colour bins. This allows us to find a distribution of the number of stars along a magnitude bin in bins of colour. We obtain a distribution histogram for the number of stars in each magnitude bin.
- Each one of these histograms is fitted by a Gaussian function and we obtain for this function its maximum height (A), its central value (x_0) and its standard deviation (σ).
- The fiducial line is formed from the points with coordinates (x_0, m_0) where m_0 is the average magnitude in each magnitude bin.

Table 9 presents the FL derived by Sarajedini (1992) (Columns 1 and 2), that derived by us in this paper (Columns 3, 4 and 5), an eyeball fit to our FL (Columns 6 and 7) and an eyeball fit to the Sarajedini (1992) CMD made by us (Columns 8 and 9). Tables 10 and 11 give the colours, magnitudes and colour dispersion for the fiducial lines, calculated with the procedure described above, for the B vs $(B - V)$ and V vs $(V - I)$ colour magnitude diagrams.

Figure 5 presents the FL derived by Sarajedini (1992) (blue) from an eyeball fitting to the points on his CMD and the FL we derived in this paper (red) following the procedure described above. We have also included in this figure an eyeball fit to our FL (pink), as well as an eyeball fit made to the CM diagram of Sarajedini's made by us (green). The FL we derived using the Gaussian technique has errors in the $(B - V)$ colour that bring it in close agreement with the Sarajedini (1992) fiducial line. However, in the magnitude range $14.0 \leq V \leq 16.0$ our fiducial line appears ≈ 0.1 units bluer than that of Sarajedini's. Even if we consider the estimated error for the $(B-V)$ colour of our observations (≈ 0.03) this cannot explain a shift of this magnitude. Fainter than $V \approx 16.0$ and down to $V \approx 19.0$ our FL and that

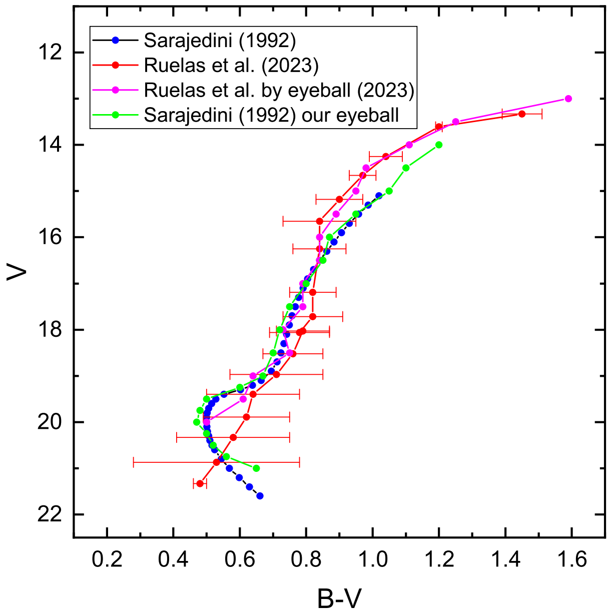

Fig. 5. The blue dots show the fiducial line derived by Sarajedini (1992) from an eyeball fit to his CMD. The red dots show the FL derived in this paper following the procedure described herein (see text); error bars for these points are also shown. The pink dots show an eyeball fit to our FL and finally, the green dots show an eyeball fit to the Sarajedini CMD made by us. The colour figure can be viewed online.

of Sarajedini's coincide within the errors. Further down than $V \approx 19.0$ there is again a discrepancy which, in this case, is simply due to the paucity of our data at these faint magnitudes.

The difference we observe between our FL and that of Sarajedini's at brighter magnitudes baffles us and we cannot find, at this point, a reasonable explanation for it. Our observations are quite incomplete at levels deeper than $V \approx 19$; that is why our FL shows neither the turn-off point nor the beginning of the main sequence.

5. COLOUR-MAGNITUDE DIAGRAMS

Figure 6 shows the colour-magnitude diagrams B vs $B-V$, V vs $B-V$, V vs $V-I$ and I vs $V-I$. The lines show the fiducial Line (FL) obtained following the procedure described above and the FL displaced one and two standard deviations. We can say that those stars that lie outside the 2σ limit and do not belong to the horizontal branch of the cluster have a very low probability ($\approx 5\%$) of belonging to the globular cluster.

Figure 7 presents the colour-magnitude diagrams corresponding to the following combinations of magnitude and colour: V vs $(V-R)$, R vs $(V-R)$, R vs $(R-I)$ and I vs $(R-I)$. On these diagrams we have not drawn the fiducial lines, but they can be easily obtained following the procedure described above.

On all the colour-magnitude diagrams presented here we can clearly appreciate the presence of the giant branch (GB) which, on the V vs $B-V$ diagram extends from $V \approx 13.5$ to $V \approx 20$ where the main sequence (MS) appears to begin. Our observations are not sufficiently deep to allow us a clear detection of the MS of this cluster. However, on the V vs $V-R$ diagram we see stars that extend down to magnitude $V \approx 22$, where the turn-off point (TO) and the beginning of the MS are more clearly shown on this diagram. It is also clear that there is a number of stars that most probably do not belong to the globular cluster and that most certainly are foreground and to a lesser extent background stars. As mentioned above, the FLs obtained for three of the colour-magnitude diagrams permit us to eliminate with a high degree of certainty those stars which are located far away from the calculated fiducial line for the cluster. Below the HB and to the left (bluer colours) of the GB there is a large number of stars that could possibly be blue stragglers belonging to this cluster.

The giant branch (GB) of this cluster is very well delineated on the R vs $R-I$ and I vs $R-I$ diagrams and it extends from ≈ 12 to ≈ 18 magnitudes.

The presence of horizontal branch (HB) stars is obvious in all the diagrams. In those diagrams that include the R and I magnitudes, it is clear that the HB stars become fainter very quickly as we move towards bluer colours. In all our photometric catalogues we separated from the bulk of our observations the HB stars, and on each one of the colour-magnitude diagrams we explicitly state the number of HB stars belonging to this diagram.

5.1. *The Horizontal Branch*

The horizontal branch (HB) of globular cluster is an interesting region of their CM diagram because: (i) it contains RR-Lyrae variable stars which have a fixed absolute magnitude (within certain restrictions). This fact is tremendously useful in the calculation of the distance of the globular cluster in question. (ii) It also presents groups of red and blue HB stars and the relative number of these red and blue stars is related to the helium abundance of the stars in the cluster.

In Table 12 we give the mean value of the magnitude values for the stars in the horizontal branch for each filter with which we observed. We shall later use these values in order to calculate a distance to

TABLE 9

FIDUCIAL LINES FOR V VS (B-V)

$(B-V)_{Sa}$	V_{Sa}	$(B-V)_O$	V_O	σ_O	Eye $(B-V)_O$	Eye V_O	Eye $(B-V)_{Sa}$	Eye V_{Sa}
1.019	15.1	1.45	13.33	0.06	1.59	13	1.2	14
0.987	15.3	1.2	13.61	0.01	1.25	13.5	1.1	14.5
0.958	15.5	1.04	14.25	0.05	1.11	14	1.05	15
0.93	15.7	0.97	14.66	0.04	0.98	14.5	0.95	15.5
0.906	15.9	0.9	15.18	0.07	0.95	15	0.87	16
0.884	16.1	0.84	15.65	0.11	0.89	15.5	0.85	16.5
0.862	16.3	0.84	16.25	0.08	0.84	16	0.8	17
0.84	16.5	0.82	17.19	0.07	0.84	16.5	0.75	17.5
0.822	16.7	0.82	17.72	0.09	0.79	17	0.72	18
0.804	16.9	0.78	18.06	0.09	0.79	17.5	0.7	18.5
0.791	17.1	0.79	18.03	0.08	0.73	18	0.67	19
0.777	17.3	0.76	18.52	0.09	0.75	18.5	0.6	19.25
0.767	17.5	0.71	18.97	0.14	0.64	19	0.5	19.5
0.757	17.7	0.64	19.4	0.14	0.61	19.5	0.48	19.75
0.749	17.9	0.62	19.89	0.13	0.5	20	0.47	20
0.741	18.1	0.58	20.33	0.17			0.5	20.25
0.733	18.3	0.53	20.87	0.25			0.52	20.5
0.724	18.5	0.48	21.33	0.02			0.56	20.75
0.712	18.7						0.65	21
0.695	18.9							
0.664	19.1							
0.638	19.2							
0.602	19.3							
0.552	19.4							
0.528	19.5							
0.515	19.6							
0.506	19.7							
0.502	19.8							
0.5	19.9							
0.5	20							
0.501	20.1							
0.503	20.2							
0.506	20.3							
0.51	20.4							
0.516	20.5							
0.524	20.6							
0.544	20.8							
0.569	21							
0.598	21.2							
0.629	21.4							
0.661	21.6							

NGC 5897. We also indicate the value of the median colour of the stars in the HB. It is clear that on all the CMD the median colour is located very much towards the blue edge of the HB, indicating that the majority of the stars in the HB branch are blue stars as mentioned in Sarajedini (1992).

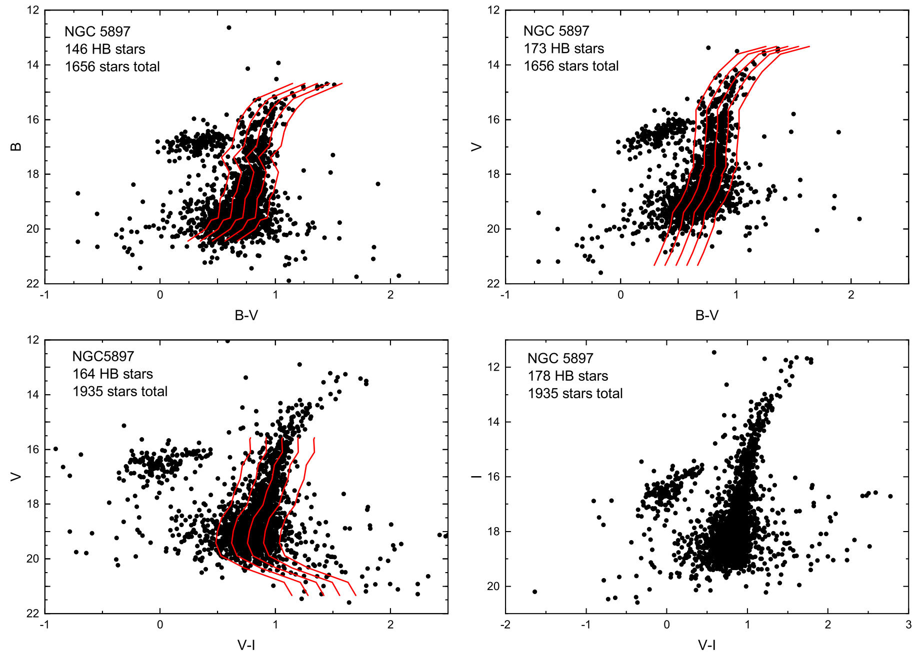

Fig. 6. Colour-magnitude diagrams for B vs $B-V$, V vs $B-V$, V vs $V-I$ and I vs $V-I$. The central red line is the fiducial line (FL) (see text) and the other red lines indicate a 1σ and 2σ separation from the FL. The estimated errors are ≈ 0.02 for the magnitudes and ≈ 0.03 for the colours, smaller than the dots representing the stars. The colour figure can be viewed online.

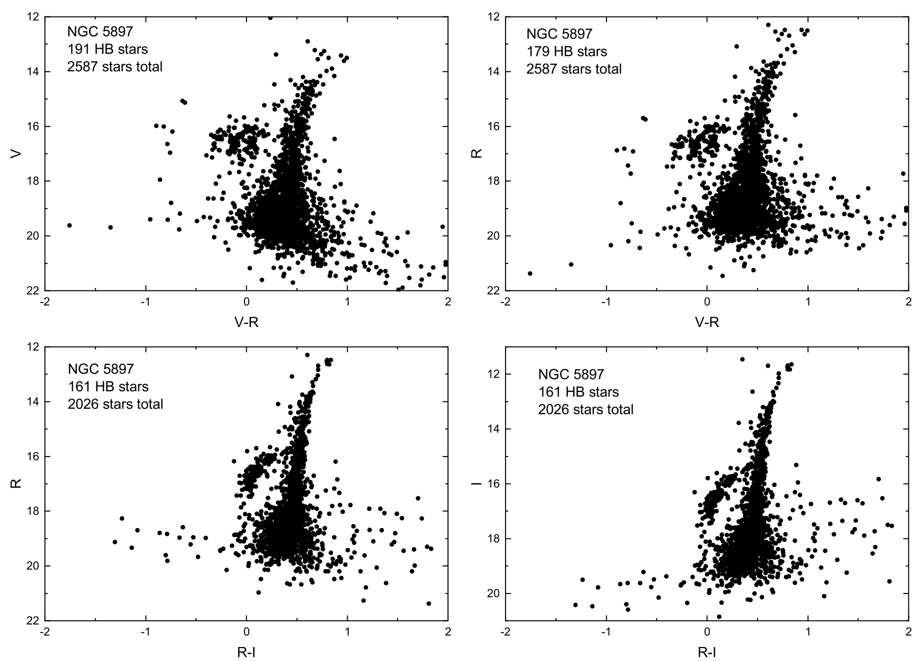

Fig. 7. Colour-magnitude diagrams for V vs $V-R$, R vs $V-R$, R vs $R-I$ and I vs $R-I$. The estimated errors are ≈ 0.02 for the magnitudes and ≈ 0.03 for the colours, smaller than the dots representing the stars.

6. METALLICITY AND REDDENING

The metallicity and the reddening of a globular cluster may be determined simultaneously by the Sarajedini method (Sarajedini, 1994 and Sarajedini & Layden, 1997), which takes into consideration the shape of the red giant branch (RGB), the observed

TABLE 10

FIDUCIAL LINE FOR B VS $(B-V)$

$B-V$	B	σ
1.365	14.683	0.106
1.05	15.238	0.068
0.968	15.608	0.085
0.895	16.078	0.098
0.864	16.444	0.113
0.838	16.969	0.081
0.747	17.382	0.019
0.814	17.925	0.073
0.773	18.639	0.102
0.737	18.888	0.055
0.731	19.248	0.12
0.718	19.592	0.253
0.656	19.682	0.151
0.611	19.993	0.143
0.456	20.441	0.138

TABLE 11

FIDUCIAL LINE FOR V VS $(V-I)$

$V-I$	V	σ
1.544	13.325	0.092
1.616	14.177	0.211
1.314	14.254	0.179
1.107	15.169	0.088
1.062	15.576	0.114
1.057	15.641	0.093
1.062	16.109	0.058
0.992	16.574	0.078
0.971	17.08	0.08
0.926	17.542	0.082
0.894	18.026	0.08
0.811	18.516	0.204
0.775	18.977	0.179
0.76	19.417	0.165
0.806	19.883	0.167
1.007	20.324	0.33
1.355	20.858	0.026
1.422	21.332	0.269

magnitude (V_{HB}) of the horizontal branch (HB), the intrinsic $(B-V)$ colour of the RGB at the level of the HB; this value will be denoted herein as: $(B-V)_{0,g}$, and the difference in observed V magnitude between the HB and the RGB at $(B-V)_{int} = 1.2$ denoted by $\Delta V_{1.2} = V_{HB\ Obs} - V_{RGB\ Obs\ at\ 1.2\ int}$, where $V_{RGB\ Obs\ at\ 1.2\ int}$ means the observed V magnitude of the RGB at an intrinsic $(B-V)$ colour equal to 1.2. Defined this way, $\Delta V_{1.2}$ results in an intrinsically positive quantity.

TABLE 12

MEAN VALUE OF THE MAGNITUDE FOR THE STARS IN THE HORIZONTAL BRANCH

CM Diagram	Mean HB Magnitude	Standard Deviation	Median Colour
B vs $B-V$	$\overline{BHB} = 16.84$	0.27	0.36
V vs $B-V$	$\overline{VHB} = 16.60$	0.46	0.37
V vs $V-R$	$\overline{VHB} = 16.57$	0.55	-0.05
R vs $V-R$	$\overline{RHB} = 16.66$	0.51	-0.05
R vs $R-I$	$\overline{RHB} = 16.63$	0.44	0.08
I vs $R-I$	$\overline{IHB} = 16.57$	0.50	0.08
V vs $V-I$	$\overline{VHB} = 16.60$	0.44	-0.01
I vs $V-I$	$\overline{IHB} = 16.58$	0.55	0.02

We applied the Sarajedini method for the stars in the V vs $(B-V)$ and the V vs $(V-I)$ colour-magnitude diagrams and obtained values for the metallicity [Fe/H] and colour excesses $E(B-V)$ and $E(V-I)$. Unfortunately, these values were completely absurd, resulting in very high metallicities and negative colour excesses. We conducted a few numerical experiments and saw that the values of the metallicity and the colour excess are very sensitive to variations of the values of the fit coefficients. The coefficients we obtained for the FLs in the V vs $(B-V)$ and V vs $(V-I)$ diagrams had errors of the order 30 % which might explain the troublesome results we obtained. We therefore decided to adopt the values given in the Harris catalogue (Harris, 1996) [Fe/H] $= -1.90$ and $E(B-V) = 0.09$.

The parameters discussed in this section could also be determined by means of isochrone fitting. There are in the literature several sets of isochrones which could be used (Girardi et al. (2002), Spada et al. (2013), `http://www.astro.yale.edu/demarque/yyiso.html`, and references therein, `http://stev.oapd.inaf.it/cgi-bin/cmd` and references therein. We shall report on this elsewhere.

7. DISTANCE MODULUS

Using the assumption that the average absolute magnitude of the HB is equal to the absolute magnitude of the RR-Lyrae stars in the cluster, we calculate the distance to the cluster we study here (for a justification of this assumption see, for example, Christy, 1966; Demarque & McClure, 1977 and Saio, 1977).

For the RR-Lyrae stars, a linear relation between absolute magnitude and metallicity of the form $M = a + b[\mathrm{Fe/H}]$ is proposed in the astronomical literature. Determination of the constants a and b is achieved using the following methods: (i) statistical parallaxes, (ii) the BBW moving atmosphere method, and (iii) main sequence fitting (Sandage & Tammann (2006)).

In the following paragraphs we shall use different absolute magnitude-metallicity relations from the literature for RR-Lyraes, which combined with the metallicity and the apparent magnitude for the HB of NGC 5897, will permit us to determine the value of its distance modulus.

A compilation of statistical parallaxes of field RR-Lyrae stars has been presented by Wan et al. (1980) in a Catalogue of the Shanghai Observatory. This compilation is summarised in Table 3 of Reid (1999). There is a value for $\langle M_{\rm V}\rangle_{\rm RR} = 0.83 \pm 0.23$ for $\langle[\mathrm{Fe/H}]\rangle$ values around -0.75 and another $\langle M_{\rm V}\rangle_{\rm RR} = 0.85 \pm 0.15$ for $\langle[\mathrm{Fe/H}]\rangle$ values around -1.56. A linear extrapolation to the metallicity of NGC 5897 ([Fe/H] = -1.90) produces a value for

$$\langle M_{\rm V}\rangle_{\rm NGC\ 5897} = 0.86\,.$$

The extrapolation process poses a problem for this determination.

Using a combination of the infrared flux and the Baade-Wesselink analysis methods Fernley et al. (1989), Fernley et al. (1990a), Fernley et al. (1990b), Skillen et al. (1989), and Skillen et al. (1993) study 21 RR-Lyrae variable stars and obtain a mean relation for their absolute magnitude expressed as follows:

$$\langle M_{\rm V}\rangle_{\rm RR} = (0.21 \pm 0.05)[\mathrm{Fe/H}] + (1.04 \pm 0.10)\,,$$

which for the metallicity value of our globular cluster produces a result of

$$\langle M_{\rm V}\rangle_{\rm NGC\ 5897} = 0.64 \pm 0.20\,.$$

Fernley (1993) uses his near-IR Sandage period-shift effect (SPSE) and a theoretical pulsation relation to derive the following relation:

$$\langle M_{\rm V}\rangle_{\rm RR} = 0.19[\mathrm{Fe/H}] + 0.84\,,$$

which applied to our cluster gives

$$\langle M_{\rm V}\rangle_{\rm NGC5897} = 0.48\,.$$

McNamara (1997) has reanalysed these same 29 stars making use of more recent Kurucz model atmospheres and derives a steeper, more luminous calibration given as follows:

$$\langle M_{\rm V}\rangle_{\rm RR} = (0.29 \pm 0.05)[\mathrm{Fe/H}] + (0.98 \pm 0.04)\,,$$

The RR-Lyraes studied in the McNamara paper belong to a metallicity interval from approximately -2.2 to 0.0. The metallicity value for our globular cluster (-1.90) lies within this interval, making it reasonable to apply this relation to this cluster. The value we obtain from this relation is:

$$\langle M_{\rm V}\rangle_{\rm NGC\ 5897} = 0.43 \pm 0.14\,.$$

Tsujimoto et al. (1998) have analysed data for 125 *Hipparcos* RR Lyraes in the metallicity range $-2.49 < [\mathrm{Fe/H}] < 0.07$ using the maximum likelihood technique proposed by Smith (1988). This technique allows simultaneous correction of the Malmquist and Lutz-Keller biases, allowing a full use of negative and low-accuracy parallaxes. They derive the following relation:

$$\langle M_{\rm V}\rangle_{RR} = (0.59{\pm}0.37) + (0.20{\pm}0.63)([\mathrm{Fe/H}]+1.60)\,.$$

Given that $[\mathrm{Fe/H}]_{\rm NGC\ 5897} = -1.90$ is contained within the studied metallicity interval, applying this relation to the cluster studied in this paper produces

$$\langle M_{\rm V}\rangle_{\rm NGC\ 5897} = 0.53 \pm 0.56\,.$$

Arellano Ferro et al. (2008) using the technique of Fourier decomposition for the light curves of RR-Lyraes in several globular clusters derive the following relation:

$$\langle M_{\rm V}\rangle_{\rm RR} = +(0.18 \pm 0.03)[\mathrm{Fe/H}] + (0.85 \pm 0.05)\,.$$

This relation was obtained for a set of globular clusters contained within the metallicity interval $-2.2 < [\mathrm{Fe/H}] < -1.2$ making it appropriate for the metallicity value (-1.90) we have for NGC 5897.

Applying this relation to our cluster we find

$$\langle M_{\rm V}\rangle_{\rm NGC\ 5897} = 0.51 \pm 0.10\,.$$

There are many different empirical and theoretical determinations of the $\langle M_{\rm V}\rangle - [\mathrm{Fe/H}]$ relation for RR-Lyrae stars, for ample discussions see Chaboyer (1999), Cacciari & Clementini (2003) and Sandage & Tammann (2006). Determining which one is the most appropriate for NGC 5897 is beyond the scope of this paper, so we have decided to consider all of them for the calculation of the distance modulus of the globular cluster studied in this paper.

From the data presented in this paper we determine an apparent V magnitude for the HB of NGC 5897 of 16.60 ± 0.46, which combined with the values for the absolute magnitudes of the RR-Lyrae

TABLE 13

DISTANCE MODULUS FOR NGC 5897

From the calibration given in	$\langle M_V \rangle$	$(m-M)_0$ $m_{HB} - \langle M_V \rangle - 3.1E(B-V)$
Wan et al. (1980)	0.86 ± 0.10	15.66 ± 0.10
Fernley (1993)	0.48 ± 0.10	16.04 ± 0.10
Skillen et al. (1993)	0.64 ± 0.20	16.08 ± 0.20
McNamara (1997)	0.43 ± 0.14	16.17 ± 0.14
Tsujimoto et al. (1998)	0.53 ± 0.56	16.91 ± 0.56
Arellano Ferro et al. (2008)	0.51 ± 0.10	16.01 ± 0.10

stars and the assumption that the HB and the RR-Lyraes have the same absolute magnitude yields the distance modulus values presented in Table 13.

A weighted average (by the inverse square of the errors) of these values results in an average distance modulus for NGC 5897 of 15.96 ± 0.64 (15500^{+5200}_{-3900} pc). The errors we encounter represent a $\approx \pm 34\%$ error in distance. For the most part the error in the distance modulus comes from the errors in the absolute magnitude versus metallicity relations (see Table 13, Column 2), and not from the errors in our photometry.

Benedict et al. (2002), using the HST parallax for the prototype RR-Lyrae star, determine an absolute magnitude for this star of $M_v = 0.61 \pm 0.10$. If we assume that the HB of NGC 5897 has this value for its absolute magnitude, then we obtain a distance modulus of:

$$(m-M)_0 = (16.60 \pm 0.46) - (0.61 \pm 0.10)$$
$$-3.1 \times (0.09 \pm 0.10) = 15.71 \pm 0.87 ,$$

which agrees, within the errors, with previous determinations. This value of the distance modulus produces a distance of 13800^{+6800}_{-4600} pc to NGC 5897 with an error of $\approx \pm 49\%$.

We adopt as our best determination for the NGC 5897 distance modulus the average of the values obtained with the Fernley (1993) (16.04 ± 0.10), and the Arellano Ferro et al. (2008) (16.01 ± 0.10) calibrations due to the fact that these calibrations present the smallest errors. This average results in 16.02 ± 0.14.

8. CONCLUSIONS

In this paper we present B, V, R and I CCD photometry for the globular cluster NGC 5897. We obtained aperture photometry for a number of standard stars in the Landolt (1992) regions, and then compared our observed stars with the magnitudes published by Stetson (1992). After aligning and matching the different sections of the globular cluster, we were able to produce magnitude catalogues for all the filters (a sample of these catalogues is presented in Appendix A). We formed eight colour magnitude (CM) diagrams (see Figures 6 and 7). In all these CM diagrams we can clearly see the red giant branch (RGB), the horizontal branch (HB) and the beginning of the main sequence (MS). Towards bluer colours from the MS turn-off point, we see a somewhat large number of stars that we identify as blue stragglers in this cluster. We tried to calculate the metallicity and the reddening of this cluster making use of the Sarajedini-Layden method (see Sarajedini (1994) and Sarajedini & Layden (1997)), but we were unable to do so. We calculated the distance modulus to this cluster, and it resulted in 16.02 ± 0.14 which corresponds to a distance of 16.0 ± 1.0 kpc.

We would like to thank the Instituto de Astronomía at Universidad Nacional Autónoma de México (IAUNAM) and the Instituto de Astronomía y Metereología at Universidad de Guadalajara (IAMUdeG) for providing a congenial and stimulating atmosphere in which to work. We also thank the computing staff at both institutions for being always available and ready to help with random problems with our computing equipment, which arise when one least expects them. We would also like to thank Juan Carlos Yustis for help with the production of the figures in this paper. We also thank Dirección General de Asuntos del Personal Académico, DGAPA at UNAM for financial support under projects PAPIIT IN103813, IN102517 and IN102617. The help and valuable suggestions provided by an anonymous referee are gratefully acknowledged.

APPENDIX

In Tables 14 and 15 we present samples of the magnitude catalogues for this paper. The complete catalogues are available upon request.

TABLE 14

B and *V* MAGNITUDES STARS IN NGC 5897

x (pixels)	*y* (pixels)	Mag *B*	Mag *V*
-277.6176	547.1518	19.4144	18.689125
-260.9676	469.6858	19.8054	19.129125
-242.1806	360.0848	16.6974	16.453125
-225.8216	444.9578	18.4854	17.707125
-217.0566	868.2468	19.0594	18.111125
-211.4806	404.3458	19.1194	18.453125
-210.1306	444.8878	19.9204	19.279125
-209.5756	285.4678	18.1414	17.317125
-206.3026	784.5288	18.7414	18.202125
-203.2576	920.8858	16.9184	16.716125
-175.0646	374.1218	18.1674	17.363125
-174.9546	461.2768	20.1134	19.484125
-167.2466	948.8658	19.0664	18.332125
-165.9416	702.2378	15.4514	14.378125
-155.0016	218.2148	19.2874	18.574125
-154.4836	140.9378	19.7204	19.065125
-147.7006	607.6628	16.9474	16.747125
-128.4606	279.8978	16.5364	16.210125
-128.0146	868.9678	16.7764	16.562125
-120.0366	848.4458	18.8774	18.148125
-96.1348	422.0696	18.9894	18.215125
-88.0116	218.9878	16.1654	15.098125
-87.8078	424.5506	20.0354	19.468125
-85.0406	473.5338	19.1244	18.368125
-83.6186	457.5028	18.6764	17.788125
-80.8708	206.5076	20.0504	19.696125
-78.9268	-112.1904	20.1914	19.493125
-77.6868	463.3066	20.2104	19.453125
-77.6686	746.1548	18.2714	17.494125
-76.6066	1057.1788	20.0354	19.186125

TABLE 15

R and *I* MAGNITUDES STARS IN NGC 5897

x (pixels)	*y* (pixels)	Mag *R*	Mag *I*
-287.2978	628.6134	16.95635	16.55932
-275.8288	546.6794	18.23635	17.89732
-253.0268	552.9184	18.94435	18.63932
-241.8808	359.8734	16.36735	16.32632
-236.2428	805.0314	18.63835	18.35832
-225.3138	444.7094	17.27135	16.85532
-216.0218	867.7194	17.56735	17.18532
-210.9128	405.2264	18.09135	17.74332
-209.2018	285.3604	16.86735	16.47632
-208.7448	670.3394	17.18435	16.76832
-208.3818	945.1264	18.31335	17.93632
-205.1298	784.2834	17.87935	17.64832
-202.7348	919.9534	16.68035	16.68832
-187.5238	817.3414	18.58435	18.19432
-184.7668	573.4634	19.30235	18.93232
-174.8078	373.8214	16.89735	16.48132
-174.5678	461.5674	19.08335	18.96432
-173.3298	625.7874	18.87335	18.70232
-166.6518	948.2634	17.86835	17.49232
-165.4968	701.9594	13.74835	13.19532
-154.6808	364.3284	18.43835	18.01332
-154.1348	218.2784	18.11335	17.87332
-153.8348	353.4634	18.91635	18.60632
-153.8298	141.3604	18.79335	19.65532
-147.3108	607.1884	16.71035	16.72932
-146.6818	407.2014	18.29635	17.68232
-140.7538	880.8234	17.97135	17.56732
-138.8768	586.5374	18.46135	17.96932
-132.2968	412.4374	18.94335	18.67032
-128.3178	279.7424	16.07935	15.98132

REFERENCES

Arellano Ferro, A., Giridhar, S., Rojas López, V., et al. 2008, RMxAA, 44, 365

Beasley, M. A. 2020, in Reviews in Frontiers of Modern Astrophysics; From Space Debris to Cosmology, ed. P. Kabáth, D. Jones, & M. Skarka (Springer International Publishing), 245, https://doi.org/10.1007/978-3-030-38509-5_9

Benedict, G. F., McArthur, B. E., Fredrick, L. W., et al. 2002, AJ, 123, 473, https://doi.org/10.1086/338087

Binney, J. & Merrifield, M. 1998, Galactic Astronomy (Princeton, NJ: PUP)

Cacciari, C. & Clementini, G. in Stellar Candles for the Extragalactic Distance Scale, ed. D. Alloin & W. Gieren (Lecture Notes in Physics 365), 105, https://doi.org/10.1007/b13985

Chaboyer, B. 1999, in Post-Hipparcos Cosmic Candles, ed. A. Heck & F. Caputo (Astrophysics and Space Science Library 237), 111, https://doi.org/10.1007/978-94-011-4734-7

Christy, R. F. 1966, ApJ, 144, 108, https://doi.org/10.1086/148593

Demarque, P. & McClure, R. D. 1977, in Evolution of Galaxies and Stellar Populations, ed. B. M. Tinsley & R. B. Larson (New Haven, CT: Yale University Observatory), 199

Fernley, J. 1993, A&A, 268, 591

Fernley, J. A., Lynas-Gray, A. E., Skillen, I., et al. 1989, MNRAS, 236, 447, https://doi.org/10.1093/mnras/236.3.447

Fernley, J. A., Skillen, I., Jameson, R. F., Barnes, T. G., Kilkenny, D., & Hill, G. 1990a, MNRAS, 247, 287

Fernley, J. A., Skillen, I., Jameson, R. F., & Longmore, A. J. 1990b, MNRAS, 242, 685, https://doi.org/10.1093/mnras/242.4.685

Ferraro, F. R., Fusi Pecci, F., & Buonanno, R. 1992, MNRAS, 256, 376, https://doi.org/10.1093/mnras/256.3.376

Girardi, L., Bertelli, G., Bressan, A., et al. 2002, A&A, 391, 195, https://doi.org/10.1051/0004-6361:20020612

Harris, W. E. 1996, AJ, 112, 1478, https://doi.org/10.1086/118116

__________. 2010, arXiv:1012.3224, https://doi.org/10.48550/arXiv.1012.3224

Harris, W. E., Harris, G. L. H., & Alessi, M. 2013, ApJ, 772, 82, https://doi.org/10.1088/0004-637X/772/2/82

Ishchenko, M., Sobolenko, M., Berczik, P., et al. 2023, A&A, 673, 152, https://doi.org/10.1051/0004-6361/202245117

Laher, R. R., Gorjian, V., Rebull, L. M., et al. 2012, PASP, 124, 737, https://doi.org/10.1086/666883

Landolt, A. U. 1992, AJ, 104, 340, https://doi.org/10.1086/116242

McNamara, D. H. 1997, PASP, 109, 857, https://doi.org/10.1086/133956

Mihalas, D. & Binney, J. 1981, Galactic Astronomy & Binney, J. (San Francisco, CA: Freeman)

Monella, R. 1985, Col, 53, 225

Palma, T. 2023, BAAA, 64, 136

Pfeffer, J., Kruijssen, J. M. D., Bastian, N., Crain, R. A., & Trujillo-Gomez, S. 2023, MNRAS, 519, 5384, https://doi.org/10.1093/mnras/stad044

Reid, I. N. 1999, ARA&A, 37, 191, https://doi.org/10.1146/annurev.astro.37.1.191

Ruelas-Mayorga, A., Sánchez, L. J., Herrera, G., & Nigoche-Netro, A. 2010, RMxAA, 46, 3

Saio, H. 1977, Ap&SS, 50, 93, https://doi.org/10.1077/BF00648522

Sandage, A. & Katem, B. 1968, ApJ, 153, 569, https://doi.org/10.1086/149687

Sandage, A. & Tammann, G. A. 2006, ARA&A, 44, 93, https://doi.org/10.1146/annurev.astro.43.072103.150612

Sarajedini, A. 1992, AJ, 104, 178, https://doi.org/10.1086/116229

__________. 1994, AJ, 107, 618, https://doi.org/10.1086/116880

Sarajedini, A. & Layden, A. 1997, AJ, 113, 264, https://doi.org/10.1086/118250

Skillen, I., Fernley, J. A., Jameson, R. F., Lynas-Gray, A. E., & Longmore, A. J. 1989, MNRAS, 241, 281, https://doi.org/10.1093/mnras/241.2.281

Skillen, I., Fernley, J. A., Stobie, R. S., & Jameson, R. F. 1993, MNRAS, 265, 301, https://doi.org/10.1093/mnras/265.2.301

Spada, F., Demarque, P., Kim, Y. C., & Sills, A. 2013, ApJ, 776, 87, https://doi.org/10.1088/0004-637X/776/2/87

Stetson, P. B. 1992, JRASC, 86, 71

__________. 2019, Canadian Advanced Network for Astronomical Photometric Standard Fields: NGC 5897, pastime visited March 19th 2022

Strader, J., Brodie, J. P., Cenarro, A. J., Beasley, M. A., & Forbes, D. A. 2005, AJ, 130, 1315, https://doi.org/10.1086/432717

Tsujimoto, T., Miyamoto, M., & Yoshii, Y. 1998, ApJ, 492, 79, https://doi.org/10.1086/311084

Wan, L., Mao, Y. Q., & Ji, D. S. 1980, Annals of the Shanghai Observatory, 2, 1

Webbink, R. F. in IAUS 113, Dynamics of Star Clusters, ed. J. Goodman & P. Hut (Princeton, NJ: Dordrecht Reidel), 541

Wehlau, A. 1990, AJ, 99, 250, https://doi.org/10.1086/115324

E. Macías-Estrada, A. Ruelas-Mayorga, and L. J. Sánchez: Instituto de Astronomía, Universidad Nacional Autónoma de México, Apartado Postal 70-264, Cd. Universitaria 04510, CDMX, México (emacias, rarm, leonardo@astro.unam.mx).

A. Nigoche-Netro: Instituto de Astronomía y Meteorología, Universidad de Guadalajara, Guadalajara, Jal. 44130, México (anigoche@gmail.com).